Consistency of two global MODIS aerosol products over ocean on Terra and Aqua CERES SSF datasets

Alexander Ignatov*[a], Patrick Minnis[b], Bruce Wielicki[b], Norman Loeb[b,c], Lorraine Remer[d], Yoram Kaufman[d], Walt Miller[b,e], Sunny Sun-Mack[b,e], Istvan Laszlo[a], Erika Geier[b]

[a]NOAA/NESDIS, Office of Research and Applications, 5200 Auth Road, Camp Springs MD 20746
[b]NASA/LaRC, Atmospheric Sciences, Hampton, VA 23681
[c]Hampton University, Center for Atmospheric Sciences, Hampton, VA 23681
[d]NASA/GSFC, Greenbelt, MD 20771
[e]Science Applications International Corporation (SAIC), Hampton, VA 23681

ABSTRACT

MODIS aerosol retrievals over ocean from *Terra* and *Aqua* platforms are available from the Clouds and the Earth's Radiant Energy System (CERES) Single Scanner Footprint (SSF) datasets generated at NASA Langley Research Center (LaRC). Two aerosol products are reported side-by-side. The *primary* M product is generated by subsetting and re-mapping the multi-spectral (0.44-2.1 μm) MOD04 aerosols onto CERES footprints. MOD04 processing uses cloud screening and aerosol algorithms developed by the MODIS science team. The *secondary* (AVHRR-like) A product is generated in only two MODIS bands: 1 and 6 on *Terra*, and 1 and 7 on *Aqua*. The A processing uses NASA/LaRC cloud-screening and NOAA/NESDIS single channel aerosol algorithm. The M and A products have been documented elsewhere and preliminarily compared using two weeks of global *Terra* CERES SSF (Edition 1A) data in December 2000 and June 2001. In this study, the M and A aerosol optical depths (AOD) in MODIS band 1 (0.64 μm), τ_{1M} and τ_{1A}, are further checked for cross-platform consistency using 9 days of global *Terra* CERES SSF (Edition 2A) and *Aqua* CERES SSF (Edition 1A) data from 13-21 October 2002.

Keywords: MODIS, aerosol optical depth, CERES, SSF.

1. INTRODUCTION

The *Terra* and *Aqua* satellites (launched in December 1999 and May 2002, respectively) carry four Clouds and the Earth's Radiant Energy System (CERES) instruments, to measure the radiant energy exchange on Earth[1]. *Terra* carries flight models 1 and 2 (FM1-2) and *Aqua* carries flight models 3 and 4 (FM3-4). The Single Scanner Footprint (SSF) products combine the CERES data with cloud and aerosol retrievals from the MODerate resolution Imaging Spectro-radiometers (MODIS), also onboard *Terra* and *Aqua*[2]. The SSF retains the mean and standard deviation of the imager pixel radiances and cloud/aerosol retrievals separately for the clear and cloudy portions of every CERES field-of-view (FOV). The spatial resolution (equivalent diameter at nadir) is 0.25-1 km for MODIS and ~20 km for CERES.

Over ocean, two aerosol products are reported side-by-side, both derived from MODIS yet using different sampling and aerosol algorithms[3]. The *primary* M product is derived from the standard MOD04 granules developed by the MODIS Science Team, whereas a simpler *secondary* AVHRR-like A product is produced by the CERES Science Team with a less sophisticated cloud clearing and a single-channel NESDIS aerosol algorithm. The A product serves as a backup for the M product. Also, it is helpful to place the 20+ year heritage AVHRR aerosol record in context of the more accurate M aerosols, and to quantify the MODIS multi-channel improvement. This study briefly describes the M and A products on the *Terra* and *Aqua* CERES SSF datasets (for more detail, see Ref. 3), and cross-compares retrievals from the two platforms using 9 days of global data from 13-21 October 2002.

2. THE M AND A AEROSOL PRODUCTS ON THE CERES SSF DATASETS

The *primary* M aerosol product on the CERES SSF is generated by subsetting and remapping the MOD04 granules onto CERES footprints. It uses sophisticated cloud screening and multispectral (0.44-2.1 μm) aerosol retrieval algorithms

*Alex.Ignatov@noaa.gov; phone (301)763-8053 ×190; fax (301)763-8572.

Passive Optical Remote Sensing of the Atmosphere and Clouds IV, edited by Si Chee Tsay, Tatsuya Yokota, Myoung-Hwan Ahn, Proc. of SPIE Vol. 5652 (SPIE, Bellingham, WA, 2004) · 0277-786X/04/$15 · doi: 10.1117/12.577927

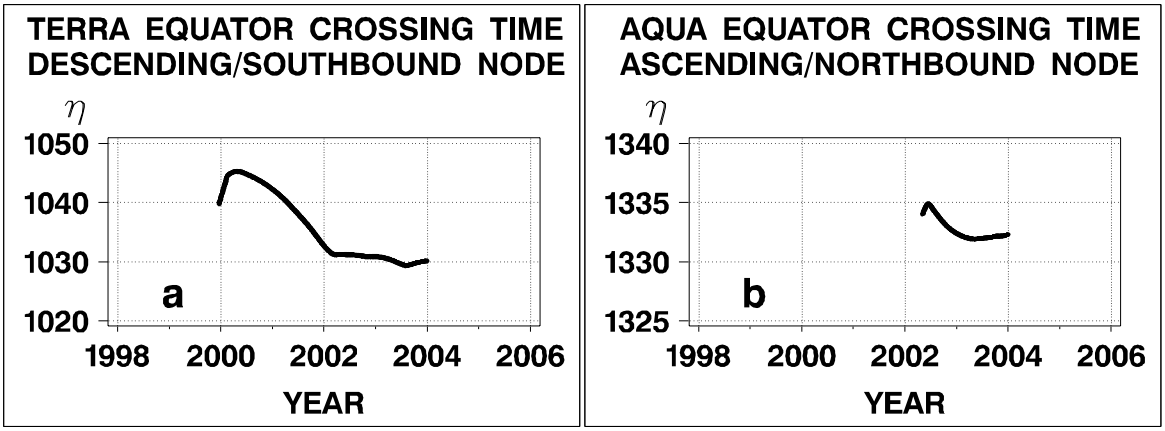

Fig. 1. Local Equator crossing time, η(h), for the *Terra* and *Aqua* platforms. Data are the two-line element from www.celestrak.com. Note that the nominal EXTs are 1030 for *Terra* and 0130 for *Aqua*. For details, see Ref. 12.

developed by the MODIS cloud and aerosol groups[4-7]. Of the 47 aerosol parameters in each MOD04 granule, 13 are saved on the CERES SSF, and of them, only one M aerosol optical depth (AOD), τ_{M1} is analyzed in this study. The τ_{M1} is reported at the centroid wavelength of MODIS band 1 (λ_1=0.644 μm).

The *secondary* A product uses different sampling (glint and cloud screening) criteria[8-9] and a simpler AVHRR-like 3rd generation NESDIS aerosol algorithm, which is currently employed operationally with AVHRR/3 on the NOAA-16 and -17 platforms[10-11]. Two AODs, τ_{A1}(0.630 μm) and τ_{A2}(1.610 μm) [τ_{A2}(2.113 μm) on *Aqua*, where band 6 is of poor quality], are derived from MODIS bands 1 and 6 [7 on *Aqua*] using single-channel algorithms. The τ_A's are reported at the wavelengths representative of band centers for a generic AVHRR sensor. In this study, only τ_{A1} is used.

In both products, sun glint area is excluded by making retrievals outside the γ=40° cone glint angle. *Additionally*, in the A product all of the solar side of the orbit is also excluded, for historical reasons. This restriction results in a reduced A sample compared to the M sample and is currently being re-evaluated.

In cross-platform comparisons, one should keep in mind the time difference between the two platforms. *Terra* is a morning platform, with a nominal equator crossing time, EXT~1030, whereas *Aqua* is an afternoon platform with the nominal EXT~0130 (Fig.1). However, the actual local solar time (LT) of aerosol observations may be within a few hours of the EXT, due to MODIS cross-scan and orbital inclinations of the platforms (Fig. 2). According to analyses in Ref. 13, the diurnal variations in the AOD over global ocean are small and should not affect results of comparisons.

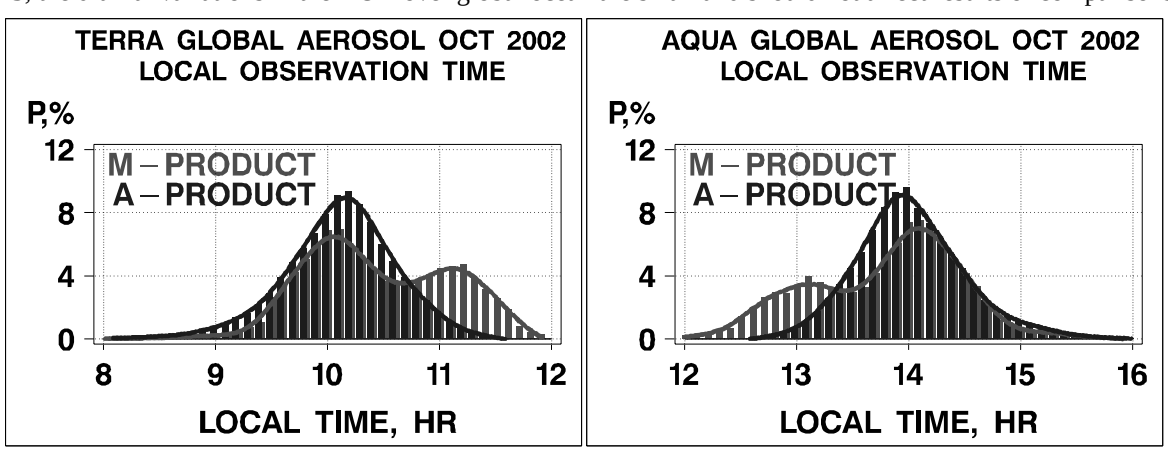

Fig. 2. Frequency of local solar time in the M and A aerosol observations from the *Terra* and *Aqua* platforms. Note that the solar side of orbit is excluded from the A product. As a result, its histogram is mono-modal and shifted with respect to the EXT towards lower sun. The second peak in the M product comes from the solar side of orbit.

Table 1. Mean statistics of τ_{1M}, τ_{1A} and auxiliary parameters in *Terra* and *Aqua* data from CERES FOVs and $(1°)^2$-boxes.

Terra/M	N	τ_{1M}	LT, h	LAT, °	LON, °	A_T, %	θ_V, °	θ_S, °	χ, °	γ, °
CERES FOVs	2,008,739	0.129	10.41	-1.2	-10.3	48.2	39.7	37.9	135.6	62.6
$(1°)^2$-boxes	164,895	0.138	10.41	-3.2	-10.9	55.3	43.2	38.3	131.7	64.3
Aqua/M	N	τ_{1M}	LT, h	LAT, °	LON, °	A_T, %	θ_V, °	θ_S, °	χ, °	γ, °
CERES FOVs	1,578,546	0.120	13.73	-3.4	-15.6	46.5	36.7	43.0	139.4	66.3
$(1°)^2$-boxes	128,996	0.124	13.72	-4.9	-14.2	54.2	41.6	44.0	134.0	68.3
Terra/A	N	τ_{1A}	LT, h	LAT, °	LON, °	A_T, %	θ_V, °	θ_S, °	χ, °	γ, °
CERES FOVs	932,810	0.133	10.17	-2.4	-7.9	32.5	32.6	37.3	149.8	64.2
$(1°)^2$-boxes	81,426	0.135	10.08	-4.1	-9.4	41.3	36.7	39.5	146.7	69.2
Aqua/A	N	τ_{1A}	LT, h	LAT, °	LON, °	A_T, %	θ_V, °	θ_S, °	χ, °	γ, °
CERES FOVs	829,467	0.130	13.90	-5.0	-13.6	30.7	30.3	41.9	152.6	68.3
$(1°)^2$-boxes	70,169	0.131	13.99	-6.4	-14.3	39.9	34.7	44.1	150.3	74.0

3. CERES SSF DATA AND MAPPING INTO $(1°)^2$ BOXES

This study uses 9 days of global M and A aerosol data from 13-21 October 2002 on the CERES/FM1 *Terra* (Edition 2A) and CERES/FM4 *Aqua* (Edition 1A) SSF datasets. The FM1 and FM4 were chosen for these analyses because they were in a cross-track mode during the 9-day period, thus facilitating geographical (co)registration of the retrievals[3].

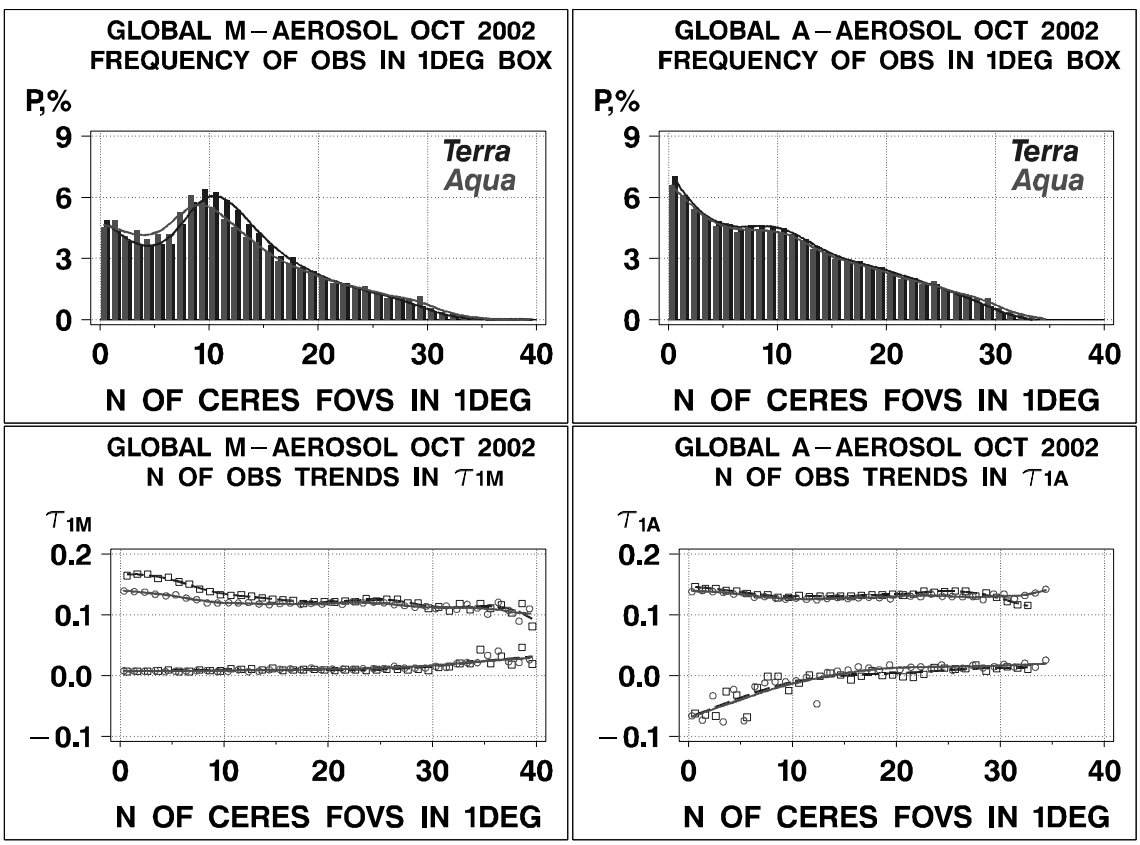

Fig. 3. Top: count of CERES FOVs in $(1°)^2$-boxes in the (left) M and (right) A products. Bottom: trends in the mean and min (left) τ_{1M} and (right) τ_{1A} from *Terra* (squares/broken lines) and *Aqua* (circles/solid lines). Note that τ_{1M} are truncated in the MOD04 processing and therefore min(τ_{1M}) never goes below zero. The τ_{1A} are not truncated and may go negative. (Physical origin of negative τ_A is discussed in Ref. 14.) Trends in τ_{1A} are smaller and more cross-platform consistent than in τ_{1M}. Close agreement between min(τ_{1A}) from *Terra* and *Aqua* MODIS bands 1indicates their excellent calibration consistency[15].

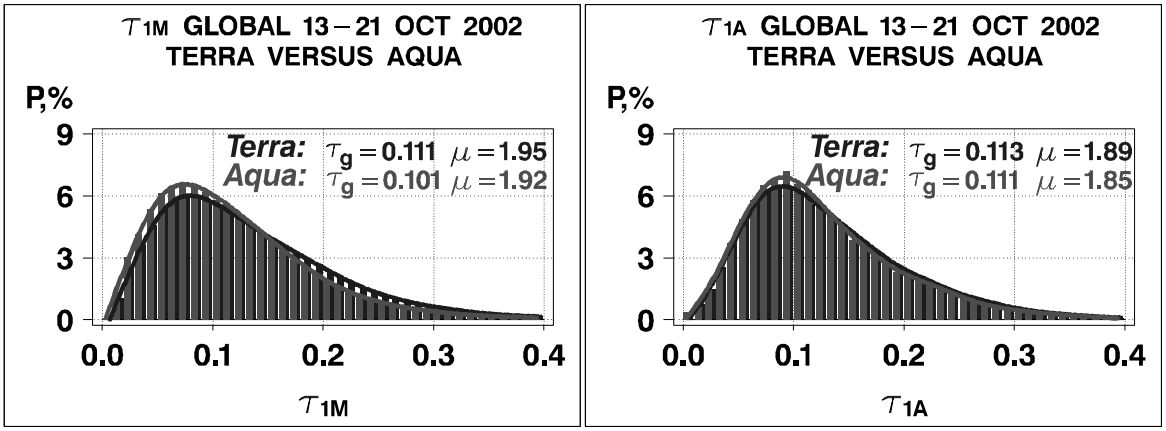

Fig. 4. Histograms of τ_{1M} and τ_{1A} derived from $(1°)^2$ *Terra* and *Aqua* data. Geometric mean and STD statistics are superimposed.

Collection 4 MOD04 *Terra* and *Aqua* products have been consistently used in the SSF processing of both datasets. In this study, we concentrate on the detailed analyses of τ-retrievals in MODIS band 1, only. Note that on the CERES SSF, the τ_{1M} and τ_{1A} are reported at slightly different wavelengths (0.644 and 0.630 μm, respectively). For the present comparisons, τ_{1A} was first re-scaled to the M wavelength of 0.644 μm as $\tau_{1A}(0.644\ \mu m) = 0.96377 \times \tau_{1A}(0.630\ \mu m)$[3].

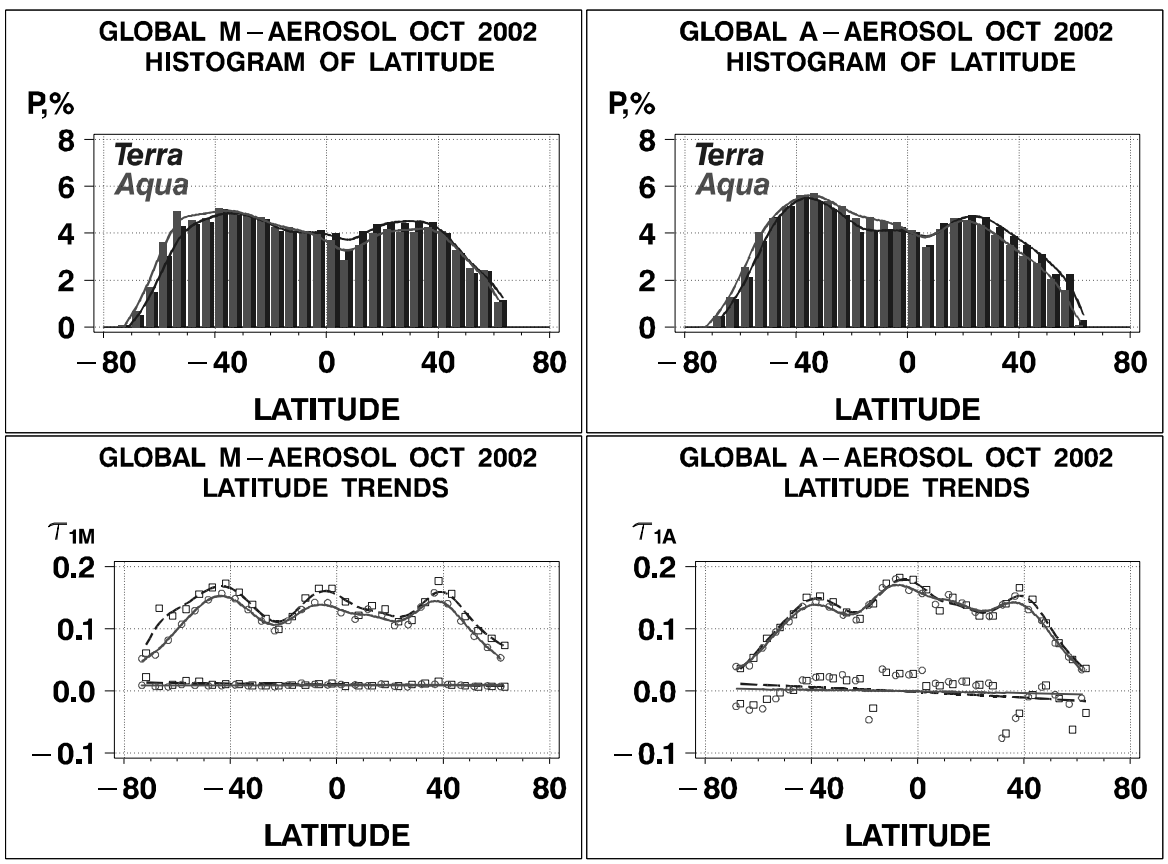

Fig. 5. Top: zonal density of M and A retrievals (bin size Δφ=5°). Spatial coverage from *Terra* and *Aqua* by M and A products is similar. Bottom: trends in the mean and min τ_{1M} (left) and τ_{1A} (right) from *Terra* and *Aqua*. (See caption to Fig.3 for detail.)

Four rows of Table 1 list counts of CERES FOVs and average statistics of the τ_{1M} and τ_{1A} from *Terra* and *Aqua*, along with the associated auxiliary parameters (local time, geography, cloud amount, and sun-view geometry). There are N=2,008,739 and N=1,578,546 CERES FOVs with τ_{1M}, and N=932,810 and N=829,467 FOVs with τ_{1A} retrievals from *Terra* and *Aqua*, respectively. In what follows, these full samples of retrievals are referred to as *products*.

To facilitate analyses below, the τ_1-retrievals and auxiliary parameters reported on the CERES FOVs have been first averaged into $(1°)^2$ boxes, resulting in N=164,895 and N=81,426 $(1°)^2$-boxes for *Terra*, and N=128,996 and N=70,169 for *Aqua* with M and A aerosols, respectively. Figure 3 (top) shows histograms of CERES FOVs counts, N, used in calculating the average statistics within each $(1°)^2$-box. Different boxes are populated non-uniformly and the shape of histograms differs for the two products, due to differences in their sampling. Smaller values of N in a box are associated with more cloud or glint, proximity to the coastal line, scan edge, or sun illumination limits.

Figure 3 (bottom) plots the respective τ_{1A}(N)-trends in the retrievals. Both τ_{1M}(N) and τ_{1A}(N) trends in Fig. 3 suggest a slight positive bias towards low N. Increased difficulties are expected in a product when approaching the boundaries of its valid domain. Note however that the τ_{1A} trends are flatter and more cross-platform consistent. A prominent feature of Fig.3 is a progressive divergence between the *Terra* and *Aqua* τ_{1M}'s towards low N, possibly indicating residual cross-platforms differences in their respective cloud screenings. These differences may result from e.g. subtle calibration differences in those MODIS bands that are used in cloud clearing but not in aerosol retrievals (e.g. thermal IR bands).

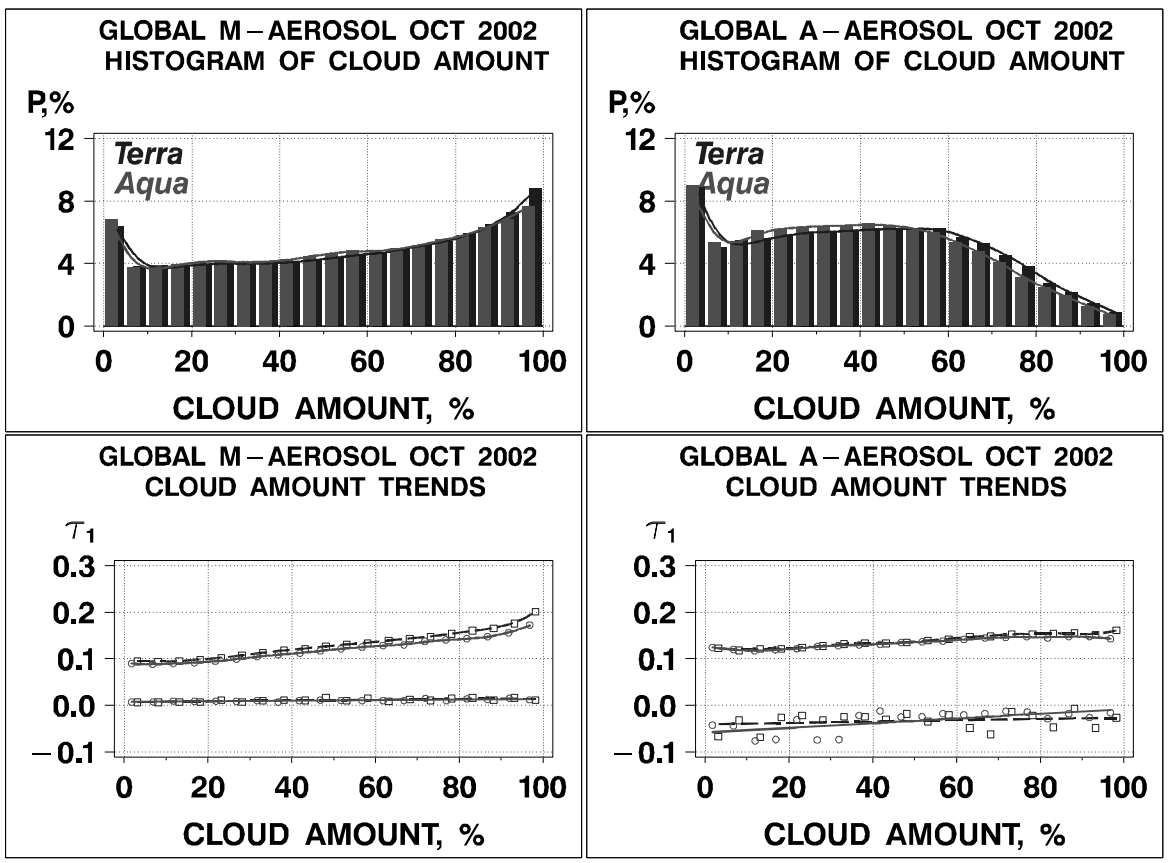

Fig. 6. Same as in Fig.5 but for the ambient cloud amount, A_T (binned at ΔA_T=5%). (Note that A_T was determined by the A-cloud screening). In the M product, maximum of the A_T-histograms is found in the highest bin centered at A_T~97.5%, whereas in the A-product, it is in the lowest bin at A_T~2.5%. As a result, the average A_T~47% in the M products compared to A_T~32% in the A-product (cf. data in Tables 1-2). Also, the τ_{1A}-trends are smaller compared to τ_{1M} trends, and more reproducible cross-platform. Small divergence between the two τ_{1M} trends increasing towards larger A_T's may indicate residual cloud screening differences in the M product between the two platforms (cf. τ_{1M}(N) trends in Fig. 4).

Table 2. Average statistics of τ_{1M}, τ_{1A} and auxiliary parameters in the *Terra/Aqua* intersection data sets for the M and A products.

Terra/Aqua M	N	τ_{1M}	LT, h	LAT, °	LON, °	A_T, %	θ_V, °	θ_S, °	χ, °	γ, °
Terra	85,985	0.131	10.45	-1.1	-17.4	53.5	41.8	40.0	130.1	63.6
Aqua	85,985	0.120	13.64	-1.1	-17.4	52.2	40.9	44.9	132.0	67.1
Terra/Aqua A	N	τ_{1A}	LT, h	LAT, °	LON, °	A_T, %	θ_V, °	θ_S, °	χ, °	γ, °
Terra	26,089	0.123	10.07	-4.3	-20.7	38.0	36.5	40.3	145.7	69.1
Aqua	26,089	0.120	13.97	-4.3	-20.7	35.6	34.1	45.2	148.3	74.0

Global average statistics of τ_1 and auxiliary parameters based on the $(1°)^2$-data are also listed in Table 1. They differ systematically from their CERES FOVs-based counterparts. In this study, we concentrate on the analyses of the $(1°)^2$-data, assuming that the effect of spatial scale does not corrupt the cross-platform comparisons, as long as consistent sampling/statistics are used in the two datasets. However, the fact that the sample statistics are sensitive to the specific way the sampling and/or averaging are done clearly indicates a need for better understanding and proper handling. Recall that both aerosol products on the CERES SSF are themselves statistics derived from pixel-level MODIS data. The derivation may be complex and involve more than one sampling and/or averaging step. For instance, the A product on the CERES SSF is derived from (sub-sampled) pixel level MODIS data, whereas the M product is derived from the 10km MOD04 product, which is itself a complex statistic derived from MODIS pixel level data[3].

4. M AND A PRODUCTS FROM TERRA AND AQUA AT A GLANCE

The global average AODs derived from $(1°)^2$-data and listed in Table 1, are τ_{1M}=0.129 and τ_{1A}=0.133 for *Terra*, and τ_{1M}=0.120 and τ_{1A}=0.130 for *Aqua*. Figure 4 plots the respective τ_1-frequency distributions. Their shape is close to log-normal[14,16]. Geometric τ-statistics are also superimposed in the graphs. All mean τ_1's (from either M or A product, *Terra* or *Aqua* platform, in both arithmetic and geometric statistics) are within ~0.01 of each other.

Figure 5 shows zonal densities and trends in the retrievals. They are closely reproducible from the two platforms, with *Terra* being slightly higher than *Aqua*. The cross-platform differences are smaller and more localized in the A product.

The data in Table 1 suggest that some auxiliary parameters associated with the retrievals may systematically differ between the M and A products. For instance, the average ambient cloud amount is A_T~55% in the M and only ~40% in the A product. Figure 6 plots the retrieved τ's as functions of cloud amount. The sensitivity is significant in both products. Similar cloud-aerosol correlations have been previously observed in the AVHRR[17], VIRS[18] and most recently in the *Terra*/MODIS[3] data. The correlation may be due to the real cloud-aerosol interactions. However the fact that the shape and magnitude of the $\tau(A_T)$ trends are product- and platform-specific suggests that residual cloud contamination may significantly contribute to the observed trends. To that end, the divergence of the $\tau_{1M}(A_T)$ trends between *Terra* and

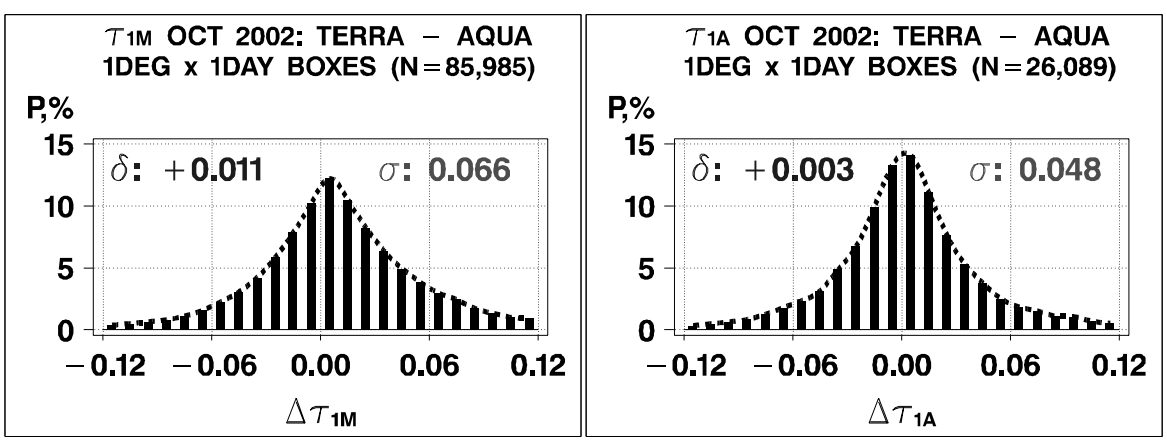

Fig. 7. Histograms of cross-platform τ_{1M} and τ_{1A}-differences derived from $(1°)^2$ Terra-Aqua match-up datasets in Table 2. Mean and STD statistics are superimposed. Note that τ_{1A} shows lower cross-platform bias and smaller RMSD.

Table 3. Average statistics of τ_{1M}, τ_{1A} and auxiliary parameters in the MA intersection data sets for *Terra* and *Aqua*.

MA Terra	N	τ_{1M}/τ_{1A}	LT, h	LAT, °	LON, °	A_T, %	θ_V, °	θ_S, °	χ, °	γ, °
M	79,209	0.123	10.17	-4.2	-9.7	46.4	37.5	39.0	144.7	67.6
A	79,209	0.134	10.07	-4.2	-9.7	41.1	36.9	39.4	146.8	69.3
MA Aqua	N	τ_{1M}/τ_{1A}	LT, h	LAT, °	LON, °	A_T, %	θ_V, °	θ_S, °	χ, °	γ, °
M	67,330	0.117	13.93	-6.6	-14.7	44.9	35.5	43.6	148.4	72.4
A	67,330	0.130	13.99	-6.6	-14.7	39.5	34.9	44.0	150.4	74.2

Aqua at large A_T may result from residual cross-platform cloud screening differences (cf. also the diverging trend in the $\tau_{1M}(N)$ at low N in Fig. 5). Note that some differences between the absolute values of the τ-retrievals and cloud amounts from the morning and afternoon platforms may exist, due to a few hours time lag. However the $\tau(A_T)$ relationship is expected to hold from platform to platform for the same product, irrespective of the physical mechanism(s) underlying this relationship. Recall that many of the current cloud screening procedures (including those used in the M and A aerosol production) are threshold-based. Therefore they may not adequately treat the cloud-aerosol transition zone, which is deemed to be largely a continuous rather than a discrete process.

5. REFINED SPACE TIME MATCHUP IN THE PRODUCT COMPARISONS

In plotting Figures 3-6, a tacit assumption was made that the whole globe, during the 9-day period, is a uniform and stable target. No specific attempt was made to precisely match the *Terra* and *Aqua* data in space and time. For analyses in this section, the $(1°)^2$ data from *Terra*/*Aqua*, and M/A products have been merged by latitude, longitude, and day.

5.1 *Terra* versus *Aqua* comparison

Cross-platform comparisons are useful to determine if the global aerosol is captured consistently from the two satellites. Table 2 shows that the M product is available from both *Terra* and *Aqua* in N=85,985 $(1°)^2$ boxes, whereas the A product is available from both platforms on the same day in only N=26,089 boxes. These two sub-samples of the full M and A products are termed the M and A *Terra/Aqua* intersections, respectively. In Figs.7-8, data from the two intersections are plotted as histograms of the *Terra-Aqua* differences and *Terra* vs. *Aqua* scattergrams. Overall, the A product shows more cross-platform consistency compared to the M product. This manifests itself in a smaller cross-platform bias (0.003 vs. 0.011) and RMSD (0.048 vs. 0.066), and in a higher cross-platform correlation (0.80 vs. 0.72).

5.2 M versus A comparison

Table 3 shows that there are N=79,209 data points in which both the M and A products are available from *Terra*, and N=67,330 such data points from *Aqua*. Figure 9 plots histograms of the "A minus M" differences. The two products show a systematic bias of $(\tau_{1A}-\tau_{1M})\sim+0.012\pm0.001$ with an RMSD from 0.039-0.045. These M-A biases are larger than

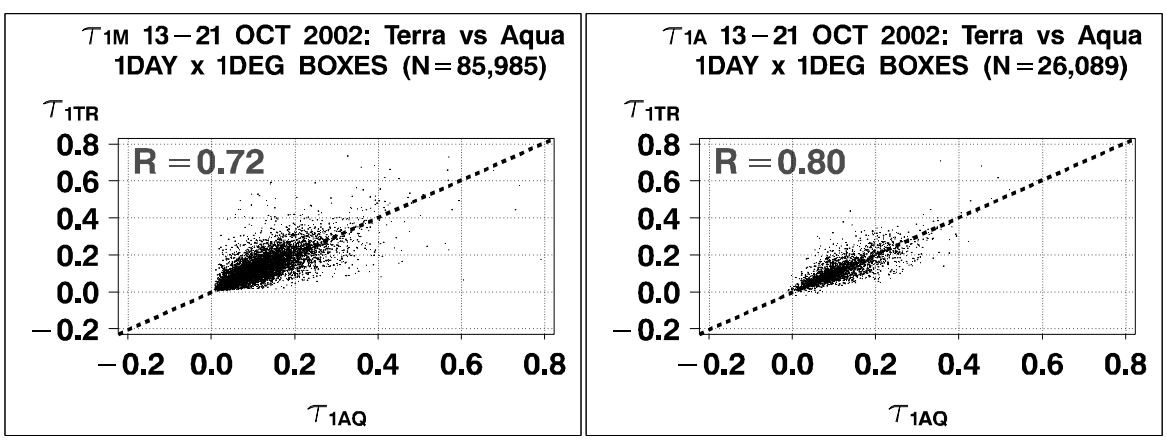

Fig. 8. Scattergrams "Terra vs. Aqua" for τ_{1M} (left) and τ_{1A}(right). The linear regression coefficients are also superimposed. Note that cross-platform correlation is higher in τ_{1A}-product.

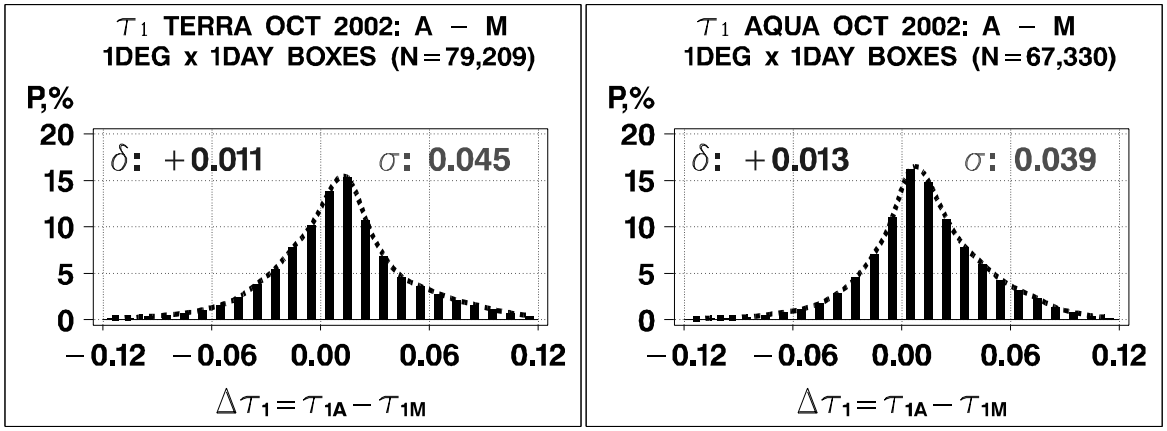

Fig. 9. Histograms of (τ_{1A}-τ_{1M}) differences derived from $(1°)^2$ (left) *Terra* and (right) *Aqua* MA-*intersection* sub-samples. The τ_{1A} shows a positive bias with respect to τ_{1M} of ~012.

the (τ_{1A}-τ_{1M})~$(4\pm5)\times10^{-3}$ differences observed in the previous *Terra* Edition 1A MA-comparisons in December 2000 and June 2001[3]. This change is deemed to be due to the use in this study of a newer version of the CERES SSF data, which is based on the MOD04 collection 4 used in the M-production. The A-processing uses a different sampling of 1km data (every 4th pixel and every other scan line in Ed2A versus every other pixel and every other scan line in Ed1A, which might affect the results of the uniformity test[18]), and more accurately defined solar flux constants. The M and A products remain highly correlated (Fig.10). The correlation coefficient is R~0.86 from both platforms (cf. R~0.84 and ~0.78 obtained in Ref.3 for Terra Edition 1A data from December 2000 and June 2001).

In Ref. 3, the MA-intersection sub-sample was used to highlight the M-A aerosol algorithm differences as sampling differences are minimized here. Note however that they are not removed completely. For instance, Table 3 shows that the average cloud amount in the MA-intersection is higher in the M product than in the A product: 46.4% versus 41.1% for *Terra*, and 44.9% versus 39.5% for *Aqua*. This is due to the fact that different MODIS pixels are sampled by the M and A products, even within the same $(1°)^2$-box.

5.3 Statistical representativeness of the intersection sub-samples

In matching the two data sets being compared as closely as possible in space and time, one must ensure that the intersection sub-sample remains representative of the full datasets. If the condition of statistical representativeness is not met, then the results of comparison cannot be extended to the full datasets.

For example, comparison of Tables 1 and 3 suggests that the *Terra* MA intersection (N=79,209) is ~97% and 48% of

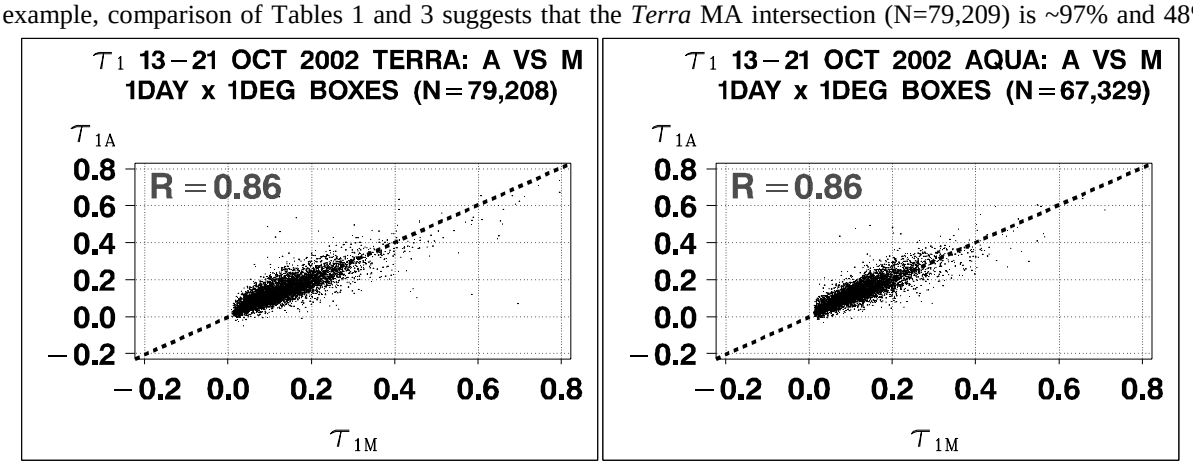

Fig. 10. Scattergrams "τ_{1A} vs. τ_{1M}" for (left) *Terra* and (right) *Aqua*. The linear regression coefficient, R, is also superimposed. (Cf. values of R~0.84 and ~0.78 obtained in Ref. 3 for two Terra datasets in December 2000 and June 2001, respectively.)

the full A (N=81,426) and M (N=164,895) samples, respectively. One might expect that that the MA-intersection here is representative of the A product, because of their 97% match. Indeed, the A product statistics (retrievals and auxiliary parameters) are very close in the full A dataset and the MA-intersection sub-sample: the average τ_{1A}=0.135 in the full set vs. τ_{1A}=0.134 in the intersection, cloud amounts are 41.3% versus 41.1%, etc. The MA-intersection is thus representative of the full A product, and all results obtained in the MA-intersection sub-sample hold for the full A dataset. On the other hand, it is not fully representative of the M product: the average τ_{1M}=0.133 in the full set versus only τ_{1M}=0.123 in the intersection, cloud amounts are 55.3% versus 46.4%, etc. Extending statistical conclusions obtained in the MA intersection to the full M sample are not justified here.

The requirement of statistical representativeness is important in many remote sensing applications such as e.g. the validation of satellite products against ground-based sun-photometers[19-20]. It is often overlooked that the comparisons are done in a relatively small intersection sample, in which both satellite and ground-based data are available. This satellite/surface intersection sample may not be representative of either satellite or sun-photometer product. Certain regions and seasons that are available in the satellite product are never covered by ground-based measurements (e.g., many areas in the open ocean, especially in the high latitudes). On the other hand, there may be domains of sun-photometer measurements that are never observed from a satellite. The intersection sub-samples, in which both satellite and ground-based product are present, may differ statistically significantly from the full samples. Analyses in this section demonstrate that it is relatively easy to check the statistical equivalency of the intersection sub-sample and the full dataset. As of the time of this writing, we are not aware of any validation studies in which this check was attempted.

6. CONCLUSION

Comparisons of the two global aerosol products derived from two satellite platforms, undertaken in this study, shed additional light on the current status of aerosol retrievals, and highlight outstanding issues.

In the M product, the *Terra-Aqua* differences are larger than in the A product. The biases tend to increase in the areas which are less populated/more cloudy, suggesting that residual cross-platform cloud screening differences may be the cause rather than diurnal changes in aerosol abundance. These analyses are in agreement with the point made elsewhere that for the overall quality of an aerosol product, sampling is at least as important as the degree of sophistication and complexity of the aerosol algorithm[3]. Clearly, complex cross-compensation mechanisms between sampling and aerosol algorithms take place in the M and A products, counter-balancing each other and leading to relatively small differences between the two global products. Presently, these mechanisms are not fully understood.

It is felt that the current priorities in the aerosol remote sensing should be revisited. In particular, the emphasis should be redirected from the increased level of aerosol algorithm complexity towards development of more scientifically sound sampling strategies. The log-normal nature of aerosol optical depth must be considered in pursuing the optimal space-time averaging procedures. Cloud screening scheme alternatives to the current threshold-based techniques should be explored[21-22]. These efforts would eventually lead to in-depth understanding and unification of the sampling algorithms.

Satellite aerosol *products* are complex combinations of input data, sampling and aerosol algorithms. These three factors are not fully independent and may interfere in a complicated way. A comprehensive system of quality control/assurance (QC/QA) of each *global product* is thus needed that includes a set of self- and cross-consistency checks that are *global* in their nature. Examples of such checks are presented in this paper. Note that these checks are not intended to replace the customary validation against ground based sun-photometers, which is considered the ultimate test for satellite retrievals. Rather, the two techniques should be used in concert with each other. In comparing different datasets using their intersection sub-samples (cross-platform or -product comparisons, or validation against ground-truth data), one must ensure that the intersection sample is statistically representative of the full data set being compared/validated.

ACKNOWLEDGEMENT

The MOD04 algorithms were developed in late 1990s by the international team of scientists (NASA/GSFC, USA, and Lab. d'Optique Atmospherique, Univ. of Lille, France), with a significant contribution from D.Tanré. The A product retrievals were initiated in late 1980s by N.Rao (deceased) and L.Stowe (retired) at NOAA/NESDIS following the pioneering ideas by M.Griggs proposed in mid-1970s. The A product has been enhanced and applied to other sensor data (TRMM VIRS, and *Terra*/*Aqua* MODIS) under the CERES project. The authors are indebted to J.Xiong,

W.Barnes, B.Guenther (NASA/GSFC-MCST), C.Moeller (Univ. Wisconsin, Madison), K.Thome (Univ of Arizona), C.Cao and J.Sullivan (NOAA/NESDIS) for helpful discussions of the MODIS radiometric issues. Help and advice from R.Hucek, S.Mattoo, A.Chu, R.Levy, R.-R.Li, V.Chiang, G.Fireman (NASA/GSFC), Q.Trepte and R.Arduini (NASA/LaRC) is also appreciated. This work was funded under the NASA EOS/CERES (NASA contract L-90987C), the NOAA/NASA/DOD Integrated Program Office, NOAA Ocean Remote Sensing, and Joint Center for Satellite Data Assimilation (NESDIS) Programs. We thank S.Mango (IPO), W.Pichel and F.Weng (NESDIS) for their support and encouragement. The *Terra* and *Aqua* CERES SSF data used in this study were obtained from the Atmospheric Sciences Data Center at NASA Langley Research Center. The views, opinions, and findings contained in this report are those of the authors and should not be construed as an official NOAA or U.S. Government position, policy, or decision.

REFERENCES

1. Wielicki B., et al, 1996: Clouds and the Earth's Radiant Energy System (CERES): An Earth Observing System Experiment. *BAMS*, **77**, *11*, 853-868.
2. Geier E., et al., 2003: CERES data management system: Single Satellite Footprint TOA/Surface fluxes and clouds (SSF) collection document. Release 2, version 1, 212 pp and appendixes http://asd-www.larc.nasa.gov/ceres/collect_guide/SSF_CG.pdf.
3. Ignatov A., P.Minnis, N.Loeb, B.Wielicki, W.Miller, S.Sun-Mack, D.Tanré, L.Remer, I.Laszlo, and E.Geier, 2004: Two MODIS aerosol products over ocean on the Terra and Aqua CERES SSF datasets. *JAS*, in press.
4. Tanré D., et al, 1997: Remote sensing of aerosol properties over oceans using the MODIS/EOS spectral radiances. *JGR*, **102**, 16,971-16,988.
5. Remer L., Y. et al, 2004: The MODIS aerosol algorithm, products, and validation. *JAS*, in press.
6. Ackerman S., et al, 1998: Discriminationg clears-sky from clouds with MODIS. *JGR*, **103**, 32139-32140.
7. Martins J., et al, 2002: MODIS cloud screening for remote sensing of aerosols over oceans using spatial variability. *GRL*, **29**, 10.1029/2001GL013252.
8. Trepte Q., et al., 1999: Scene identification for the CERES cloud analysis subsystem. *Proc. AMS 10th Conf. Atmos. Rad.*, Madison, WI, 169-172.
9. Minnis, P., et al, 2004: Daytime CERES cloud mask for non-polar regions. *JAM*, in prep.
10. Ignatov A., and L.Stowe, 2002: Aerosol retrievals from individual AVHRR channels: I. Retrieval algorithm and transition from Dave to 6S radiative transfer model. *JAS*, **59**, *3(1)*, 313-334.
11. Ignatov A., et al, 2004: Operational Aerosol Observations (AEROBS) from AVHRR/3 onboard NOAA-KLM satellites. *JTech.*, **21**, 3-26.
12. Ignatov A., et al, 2004: Equator crossing times for NOAA, ERS, and EOS sun-synchronous satellites. *Int. J. Remote Sensing*, in press.
13. Kaufman, Y., et al., 200: Will aerosol measurements form Terra and Aqua polar orbiting satellites represent the daily aerosol abundance and properties? *Geophys. Res. Lett.*, **27**, 3861-3864.
14. Ignatov, A., and L. Stowe, 2002: Aerosol retrievals from individual AVHRR channels. II. Quality control, probability distribution functions and consistency checks of retrievals. *J. Atm. Sci*, **59**, 335-362.
15. Ignatov, A., 2002: Sensitivity and information content of aerosol retrievals from AVHRR: Radiometric factors. *Appl. Opt.*, **41**, 991-1011.
16. O'Neill, N., A.Ignatov, B.Holben, and T.Eck, 2000: The log-normal distribution as a reference for reporting aerosol optical depth statistics: Empirical tests using multi-year, multi-site AERONET sun photometer data. *Geophys. Res. Lett.*, **27**, 4778, 3333-3336.
17. Ignatov, A., and N.Nalli, 2002: Aerosol retrievals from multi-year multi-satellite AVHRR PATMOS dataset for correcting remotely sensed sea surface temperature. *JTech*, **19**, 1986-2008.
18. Ignatov A., et al, 2004b: Aerosol retrievals from TRMM/ VIRS over open oceans. *JAM*, in prep.
19. Ignatov, A., L.Stowe, S.Sakerin, and G.Korotaev, 1995: Validation of the NOAA/NESDIS satellite aerosol product over the North Atlantic in 1989. *J. Geophys. Res.*, **100**, 5123-5132.
20. Remer, L., et al., 2002: Validation of MODIS aerosol retrievals over ocean. *Geophys. Res. Lett.*, **29**, 8008, doi:10.1029/2001GL013204.
21. Uddstrom, M., W.Gray, R.Murphy, N.Oien, and T.Murray, 1999: A Bayesian cloud mask for sea surface temperature retrieval. *JTech*, **16**, 117-132.
22. English, S., J.Eyre, and J.Smith, 1999: A cloud-detection scheme for use with satellite sounding radiances in the context of data assimilation for numerical weather prediction. *Q.J.R.Meteorol.Soc.*, **125**, 2359-2378.